JOURNAL OF GEOPHYSICAL RESEARCH, VOL. 105, NO. D12, PAGES 15,509-15,523, JUNE 27, 2000

Interannual variability of the tropical tropopause derived from radiosonde data and NCEP reanalyses

William J. Randel and Fei Wu
NCAR Atmospheric Chemistry Division, Boulder, Colorado

Dian J. Gaffen
NOAA Air Resources Laboratory, Silver Spring, Maryland

Abstract. Interannual variability of the tropical tropopause is studied using long time series of radiosonde data, together with global tropopause analyses from the National Centers for Environmental Prediction (NCEP) reanalyses over 1957-1997. Comparisons for the period 1979-1997 show the NCEP tropopause temperature is too warm by ~3-5 K and too high in pressure by ~2-6 mbar. However, these biases are approximately constant in time, so that seasonal and interannual variability is reasonably well captured by the NCEP data. Systematic differences in NCEP tropopause statistics are observed between the presatellite (1957-1978) and postsatellite (1979-1997) periods, precluding the use of the reanalyses for the study of multidecadal variability. Interannual anomalies in tropical average radiosonde and NCEP data show variations of order ±1-2 K over the period 1979-1997, but there can be differences between these two estimates which are of similar magnitude. These differences impact estimates of decadal trends: During 1979-1997, negative trends in tropopause temperature of order –0.5 K/decade are observed in radiosonde data but are not found in NCEP reanalyses. The space-time patterns of several coherent signals are identified in both sets of tropopause statistics. The volcanic eruption of El Chichón (1982) warmed the tropical tropopause by ~1-2 K and lowered its altitude by ~200 m for approximately 1-2 years. Smaller tropopause variations are observed following Mount Pinatubo (1991), particularly in radiosonde data. The signatures of the quasi-biennial oscillation (QBO) and El-Nino/Southern Oscillation (ENSO) events are strong in tropopause statistics. QBO variations are primarily zonal mean in character, while ENSO events exhibit dipole patterns over Indonesia and the central Pacific Ocean, with small signals for zonal averages.

1. Introduction

Coupling between the troposphere and the stratosphere by dynamical, chemical, and radiative processes is an important aspect of climate variability and global change. Of particular importance is the exchange of water, ozone, and other trace constituents between the troposphere and stratosphere (in both directions), i.e., transport across the tropopause. The tropopause marks the transition between the troposphere and the stratosphere; its most fundamental characteristic is a change in static stability (temperature lapse rate) between the troposphere (low static stability and associated fast vertical mixing time scales) and the stratosphere (high stability, slow vertical transport) [see *Holton et al.*, 1995]. This strong change in static stability is associated (outside of the tropics) with a sharp gradient in potential vorticity (PV), so that the extratropical tropopause is sometimes defined in terms of PV; the tropopause is also associated with sharp vertical gradients in constituents such as ozone, water vapor, and reactive nitrogen.

The tropical tropopause is of special importance for understanding transport of water vapor into the stratosphere. Air enters the stratosphere primarily in the tropics, where the cold tropopause temperatures lead to freeze-drying and very low water vapor mixing ratios throughout the stratosphere [*Brewer*, 1949]. Indeed, the seasonal variation in tropopause temperatures is clearly evident in the seasonal cycle of tropical stratospheric water vapor, although reconciling tropopause temperatures with observed stratospheric mixing ratios is still a matter of current research [*Mote et al.*, 1996; *Tuck et al.*, 1997; *Dessler*, 1998; *Simmons et al.*, 1999]. One requirement to understanding this transport is accurate knowledge of tropopause structure and variability.

Behavior of the global tropopause is also an aspect of the atmospheric general circulation that is not completely understood [e.g., *Thuburn and Craig*, 1997]. Outstanding problems include mechanisms which control the extratropical tropopause and the influence of extratropics on the tropical tropopause [*Thuburn and Craig*, 2000]. Also, global climate models often exhibit a persistent cold bias near the tropical tropopause [*Hamilton et al.*, 1995; *Hack et al.*, 1998]. Documentation of the climatology and variability of the tropopause from observed data is useful for characterizing and understanding such model biases. Furthermore, the tropical tropopause temperature also represents a basic potential indicator of global climate change, so that analysis of historical data contributes to quantifying such variability.

Much information on the behavior of the tropical tropopause has been derived from radiosonde data [*Reid and Gage*, 1981, 1985, 1996; *Newell and Gould-Stewart*, 1981; *Fredrick and*

Paper number 2000JD900155.
0148-0227/00/2000JD900155$09.00

Douglass, 1983; *Krishna Murthy et al.*, 1986; *Gage and Reid*, 1987; *Selkirk*, 1993]. One obvious drawback of radiosondes is the limited spatial coverage, particularly over ocean areas. An alternative is to use global meteorological analyses to identify the tropopause [*Hoerling et al.*, 1991]. *Hoinka* [1998] has recently analyzed global tropopause structure using European Centre for Medium-Range Weather Forecasts (ECMWF) reanalysis data, and *Highwood and Hoskins* [1998] and *Simmons et al.* [1999] have shown statistics derived from ECMWF operational analyses. One drawback to using such global meteorological data is that the vertical resolution is relatively coarse at upper levels, so that the derived tropical tropopause may be substantially different from results based on radiosonde data [*Highwood and Hoskins*, 1998].

The objective of this study is to examine interannual variability of the tropical tropopause based on long records of radiosonde measurements at many stations, together with global results from the National Centers for Environmental Prediction (NCEP) reanalyses [*Kalnay et al.*, 1996]. Monthly mean tropopause statistics at 26 near-tropical stations with relatively complete long-term records are obtained from a new data set compiled by D. Gaffen et al. (manuscript in preparation, 2000). These data are complemented by global fields of tropopause temperature and pressure which are output as part of the NCEP reanalysis product. Although the NCEP data span the period from 1957 to the present, there is a marked discontinuity in tropopause statistics between the presatellite (1957-1978) and postsatellite (1979 to present) periods, and we focus mainly on observed variability for the period 1979-1997. Comparisons with radiosonde data for this period shows the NCEP tropical tropopause is too warm (by ~3-5 K) and too high in pressure by ~2-6 mbar (low in altitude by ~150-450 m). However, these biases are approximately constant in time, so that the range of seasonal variability is reasonable in the NCEP statistics. Likewise, interannual variations show significant correlations between the NCEP and radiosonde data.

We use regression analyses to isolate the spatial structure of interannual variations in both radiosonde and NCEP data. The spatial structures derived from the global NCEP data provide large-scale perspective to results derived from isolated radiosonde time series. Coherent tropopause variations associated with the volcanic eruption of El Chichón [1982], the stratospheric quasi-biennial oscillation (QBO), and El Nino-Southern Oscillation (ENSO) episodes are evident and show good agreement between the NCEP and radiosonde data. However, for very low frequency tropical mean variations there can be differences of ~±1 K between the radiosonde and NCEP reanalysis estimates. Because these differences are comparable in magnitude to the signal in question, they limit confidence in estimates of decadal-scale trends. We also briefly examine coherence between the tropical tropopause and extratropical circulation and find significant interannual correlations with the stratospheric polar vortex in both hemispheres. These global correlations suggest that tropical tropopause variability is significantly influenced by the mean stratospheric Brewer-Dobson circulation.

2. Data and Analyses

2.1. NCEP Tropopause Statistics

The NCEP/National Center for Atmospheric Research (NCAR) reanalysis project uses a state-of-the-art global numerical weather analysis/forecast system to perform data assimilation using historical observations, spanning the time period from 1957 to the present [*Kalnay et al.*, 1996]. For brevity, the NCEP/NCAR reanalysis data are referred to as NCEP data throughout this paper. The model used in the NCEP reanalysis has 28 vertical levels extending from the surface to ~40 km, with vertical resolution of ~2 km near the tropical tropopause. The NCEP output includes global analyses of tropopause temperature and pressure, which are derived from temperature analyses on model sigma levels. The tropopause pressure level is defined by the standard lapse rate criterion; that is, it is identified by the lowest level (above 450 mbar) where the temperature lapse rate becomes less than 2 K/km; it is not allowed to be higher than 85 mbar. The tropopause pressure is estimated by deriving the lapse rate at each model sigma level and estimating (by interpolation in height) the pressure where the threshold value of 2 K/km is reached. Analyzed temperatures are then interpolated to this level. This algorithm produces tropopause estimates which vary smoothly in space and time. For the analysis of low-frequency variations here, we use monthly average tropopause statistics, sampled on a 5° × 10° latitude-longitude grid. The NCEP reanalysis results here extend through August 1999, but direct comparison to radiosondes covers only the period through 1997.

One motivation for the reanalysis project is to prevent temporal discontinuities in output due to model changes, such as occur when operational models are changed and improved. However, substantial changes in the reanalysis product can occur due to significant changes in input data. One large change in the NCEP reanalysis is due to the availability of global satellite data beginning in late 1978; this has a significant impact on upper air temperature in the tropics and the data-sparse Southern Hemisphere (SH) [*Mo et al.*, 1995; *Kanamitsu et al.*, 1997; *Pawson and Fiorino*, 2000; *Santer et al.*, 1999]. Comparisons with tropical radiosonde data (shown below) clearly reveal a discontinuity in NCEP tropopause statistics in late 1978, and for this reason we focus separately on the time periods 1958-1978 and 1979-1997.

2.2. ECMWF and UKMO Data

We briefly also compare tropical temperatures derived from European Centre for Medium-Range Weather Forecasts (ECMWF) reanalyses for the period 1979-1993 [*Gibson et al.*, 1997], extended through 1998 by ECMWF operational analyses. Because tropopause statistics are not produced routinely at ECMWF, we use the 100-mbar temperature analyses. These are the same data analyzed by *Simmons et al.* [1999] and are included here simply for direct comparisons to our NCEP and radiosonde results. An important detail is that the ECMWF operational analyses have undergone a series of model and assimilation changes since 1994, which may accentuate a tropopause cooling trend when compared with the pre-1993 reanalyses [*Simmons et al.*, 1999; A. Simmons, personal communication, 2000]. We furthermore include 100-mbar temperatures from the United Kingdom Meteorological Office (UKMO) stratospheric assimilation, which covers the time period October 1991 to the present [*Swinbank and O'Neill*, 1994]. Although this is a much shorter time period than that covered by the other data sets, it provides results from an independent analysis procedure. We note that fundamentally the same radiosonde and satellite observations are incorporated into the NCEP, ECMWF, and UKMO analyses, so that their differences

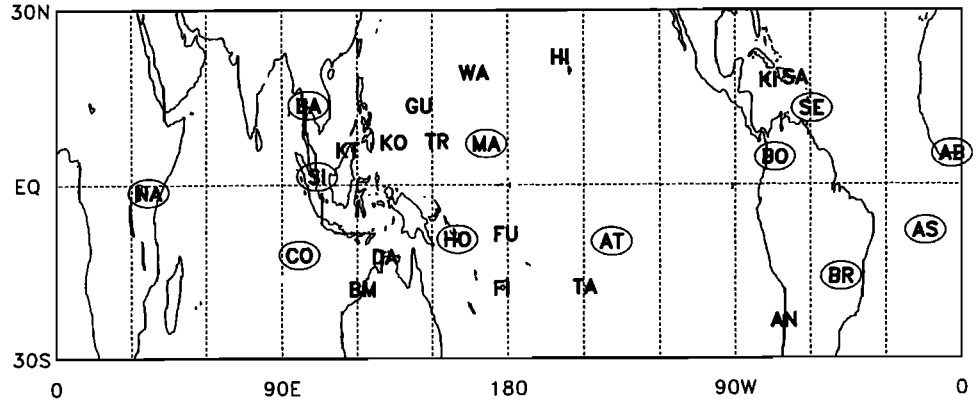

Figure 1. Locations of stations with long-term radiosonde records used in this study. The abbreviated station names are listed in Table 1 The 12 circled stations are used to estimate tropical averages in Figures 8-11.

provide a measure of the uncertainty in tropopause statistics introduced by the global analysis techniques.

2.3. Radiosonde Data

We also analyze time series of tropopause temperature and pressure derived from radiosonde observations, using a new data set prepared by D. Gaffen et al. (manuscript in preparation, 2000). That data set includes monthly statistics, based on individual sounding data, of the location of three indicators of the tropical tropopause. the standard thermal tropopause (based on a lapse-rate criterion) [*World Meteorological Organization (WMO)*, 1957]; the cold-point (or minimum temperature of the sounding); and the 100-hPa level. For each sounding, the temperature, pressure, geopotential height, potential temperature, and saturation water vapor mixing ratio were evaluated at each of these "tropopause" locations. The complete data set covers the period 1947-1997 at 94 radiosonde locations in the tropical belt (30°N-30°S) and is derived from the Comprehensive Aerological Research Data Set (CARDS) "core" network, as defined by *Wallis* [1998]. The main advantages of these tropopause data sets are that (1) use of the CARDS product maximizes the spatial and temporal coverage of the radiosonde network; (2) use of individual soundings, rather than monthly mean data, maximizes the vertical resolution for better identification of the tropopause; and (3) monthly statistics are not affected by the nonlinear relationships between observed temperature at fixed pressure levels and the temperature and pressure of the (vertically interpolated) tropopause.

Sources of error in radiosonde observations are comprehensively examined by *WMO* [1996], and here we summarize the radiosonde error characteristics relevant to the present study Pressure observations from different radiosonde types have systematic errors generally less than 1 mbar at the 100-mbar level (close to the tropical tropopause). The precision of the pressure data ranges from 0.6 to 3.5 mbar and is ≤1.6 mbar for the sonde types most commonly used at the tropical stations in this analysis. Typical systematic errors in radiosonde temperature data are about ±0.3 K at night, with precision of 0.2-0.4 K for the sonde types used in the tropics. Solar radiation effects can lead to artificial day-night differences in radiosonde temperature observations of approximately 1 K. The latter error source has been recognized for decades, and many radiosonde data processing systems include algorithms to adjust the daytime temperature data. We have computed separate 0000 and 1200 UTC monthly statistics to avoid the potential difficulties associated with changing bias characteristics in daytime and nighttime soundings or changing observing schedules. In comparisons between radiosonde data and reanalyses, differences that substantially exceed the above mentioned errors are interpreted as biases in the reanalyses.

Here we employ the monthly mean values of the temperature and pressure of the thermal tropopause (for comparison with the reanalysis tropopause) from 26 stations with relatively complete records over 1979-1997 (or longer). These stations are listed in Table 1, and their locations are shown in Figure 1. Our analyses use monthly averages of available 0000 and 1200 UTC radiosonde data, as we do not find substantial differences using either subset. We screen the monthly means by requiring that there be at least five observations within a month and that the within-month standard deviation be less than 5 K and 25 mbar for tropopause temperature and pressure, respectively.

2.4. Regression Analyses

Space-time structure of interannual anomalies in tropopause statistics are isolated using regression analyses of the form

$$T(t) = \alpha \times \text{trend} + \beta \times \text{solar} + \gamma \times \text{QBO} + \delta \times \text{ENSO}. \quad (1)$$

This functional form is chosen to allow identification of statistically significant trends, in light of known QBO and ENSO signals in tropopause behavior [e.g., *Reid and Gage*, 1985]. We use reference time series of observed QBO winds at 50 mbar (Singapore measurements updated from *Naujokat* [1986]), which tests show to be the level of best correlation with the tropopause, and the standardized ENSO or Southern Oscillation Index (SOI) updated from *Trenberth* [1984]. The solar term in (1) is a proxy for variability associated with the 11-year solar cycle, which has been identified in lower stratosphere circulation statistics [*van Loon and Labitzke*, 1994]. We find that inclusion of the solar term in (1) is significant for NCEP statistics, but not for the radiosonde data or ECMWF results. However, identification of solar variability in stratospheric data is difficult in the recent 1979-1997 record, because of aliasing with the large stratospheric warming episodes related to the El Chichón (1982) and Pinatubo (1991) volcanic eruptions. For completeness we include the solar term in all regressions, but solar variability per se is discussed only briefly here.

Table 1. Radiosonde Locations and Annual Mean Differences (NCEP Reanalysis Minus Radiosonde) in Tropopause Temperature and Pressure

Symbol	Name	Latitude, deg	Longitude, deg	Temperature Bias, K	Pressure Bias, mbar
HI	Honolulu	22	201	3.3	2.6
TA	Tahiti	-18	210	4 8	2.5
AT	Atuona	-10	221	4.4	3.0
KI	Kingston	18	283	3.4	6.2
BO	Bogota	5	286	5.3	5.9
AN	Antofagasta	-24	290	3.8	4.2
SA	San Juan	18	294	2.8	4.7
SE	Seawell	13	301	2 6	4.3
BR	Brasilia	-16	312	2 3	1.7
AS	Ascension Island	-8	346	3.7	1.6
AB	Abidjan	5	356	4.6	4.5
NA	Nairobi	-1	37	5.4	3.9
CO	Cocos Island	-12	97	5.7	2.5
BA	Bangkok	14	101	3.2	3.4
SI	Singapore	1	104	4.2	4.6
KT	Kota Kinabalu	6	116	3.8	3.1
BM	Broome	-18	122	5.2	1.8
DA	Darwin	-12	131	4.4	3.0
KO	Koror	7	134	3.7	5.7
GU	Guam	14	145	3.4	6.4
TR	Truk	7	152	3.6	6.2
HO	Honiara	-9	160	5.2	4.1
WA	Wake	19	167	3.2	5.0
MA	Majuro	7	171	3.9	6.1
FI	Fiji	-18	178	5.0	3.7
FU	Funafuti	-9	179	5.2	4.2

See Figure 1 for symbols.

As a note, we performed empirical orthogonal function (EOF) analyses of the tropical tropopause fields (over 30°N-S) to objectively isolate coherent variability. The predominant mode is coherent over ~30°N-S with little zonal structure, exhibiting time variability very similar to the zonal mean anomalies discussed below in section 4.2.1. The second and third EOF modes gave space-time structures isolating the QBO and ENSO variations discussed in sections 4.2.2 and 4.2.3. Higher-order EOF modes were not statistically significant. The dominant EOF modes yield information comparable to that shown below based on the regressions described by (1), and the choice of analysis technique is not critical.

3. Seasonal Variability

Comparisons of the mean seasonal cycle in tropopause temperature and pressure between the radiosonde and NCEP statistics are shown in Figure 2 for three widely spaced tropical stations (Bogota, Nairobi, and Truk Island). These compare the radiosonde statistics with NCEP results interpolated to the station location, for averages over 1979-1997. The radiosonde and NCEP data both show an annual cycle which is coherent throughout the tropics, with minima in temperature and pressure during Northern Hemisphere (NH) winter (December-March) and maxima during NH summer (July-September). These comparisons show the NCEP tropopause temperature has a warm bias of order 3-5 K throughout the tropics (the annual mean for each station is listed in Table 1). Likewise, the NCEP analyses show a persistent high-pressure bias of order 2-6 mbar, corresponding to an altitude which is too low by ~150-450 m. These biases are approximately constant with season, so that the seasonal cycle is reasonably well captured by the NCEP data. Moreover, there are no strong spatial patterns to the temperature or pressure biases.

Figure 3 furthermore compares the seasonal cycle behavior observed in the radiosonde and NCEP data. Figure 3a shows the amplitude of the seasonal cycle in tropopause temperature and pressure at each radiosonde station, calculated simply as the maximum minus the minimum during the year using the 1979-1997 monthly averaged statistics. These extrema occur during NH winter (December-March) and NH summer (July-September) at each station (see Figure 2); [see also *Reid and Gage*, 1981; *Fredrick and Douglass*, 1983]. The seasonal cycles shown in Figure 3 exhibit a reasonably compact scatter for most of the tropical stations, with annual variations in temperature of 4-6 K and pressure of 10-15 mbar. Notable outliers in the radiosonde data in Figure 3 are small cycles at Bangkok and in the south central Pacific (Atuona and Tahiti) and much larger annual cycles at the higher latitude stations of Honolulu (22°N), Kingston (18°N), San Juan (18°N), Wake (19°N) and Antofagasta (-24°S). The larger-amplitude seasonal cycles at these stations may suggest that they be considered subtropical rather than tropical. Note that the near-equatorial stations in Figure 3 show an approximate relationship between temperature and height variations which is close to 6 K/km.

Figure 3b shows the tropopause annual cycle in NCEP reanalysis data, sampled at the radiosonde station locations. There is reasonable agreement with the direct radiosonde estimates, with somewhat tighter grouping of the separate stations and slightly stronger overall amplitudes. The higher-latitude stations which were outliers in the radiosonde data are likewise separated in the NCEP results, except for Antofagasta (-24°S). The overall agreement is encouraging for the further analyses of NCEP results.

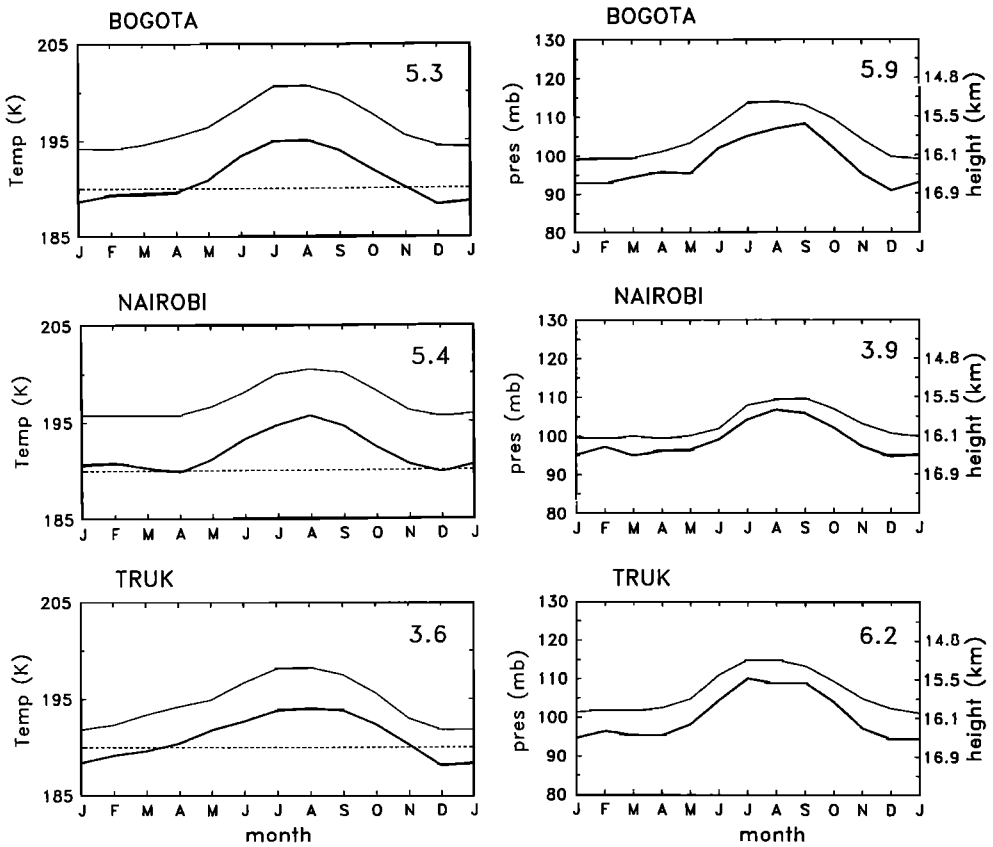

Figure 2. The mean seasonal cycle in tropopause (left) temperature and (right) pressure at Bogota, Nairobi, and Truk Island, comparing radiosonde data (bold curves) with corresponding National Centers for Environmental Prediction (NCEP) results (thin curves). The approximate (hydrostatic) height scale is included in the right-hand panels. Time average biases are listed in the upper right corner in each panel (and are listed for each station in Table 1).

For reference and comparison to other results, the 1979-1997 mean NCEP tropopause temperature fields in January and July are shown in Figure 4. The overall space-time patterns are very similar to the lapse-rate tropopause estimates given by *Highwood and Hoskins* [1998] based on ECMWF operational analyses or by *Hoinka* [1998] based on ECMWF reanalyses. In particular, January temperature minima are observed in the western Pacific warm pool region and over South America in each analysis. These January minimum NCEP temperatures of 192-194 K in Figure 3 correspond to average temperatures below 190 K when the 3- to 5-K NCEP bias is taken into account (assuming that the radiosonde values are more accurate). In July the tropical tropopause temperature has less zonal structure, and the minimum occurs over the Indian monsoon region, centered near 20°N (again, in good agreement with the ECMWF analyses). The seasonal variation of ~4-6 K seen in Figure 3 is in good agreement with radiosondes. The spatial structure of time average tropopause pressure fields derived from NCEP data is very similar to results from ECMWF data [e.g., *Hoinka*, 1998, Figure 2] and are not shown here.

4. Interannual Variability

4.1. Radiosonde-NCEP Comparisons

Interannual variations are analyzed in both the radiosonde and NCEP data by subtraction of the mean seasonal cycles, calculated as averages over 1979-1997. Figure 5 compares time series of anomalies in tropopause temperature and pressure at Truk Island over 1957-1997. This station is representative of a wide region over the western Pacific Ocean [*Reid and Gage*, 1985, 1996]. One obvious feature seen in Figure 5 is that there is a large change in NCEP tropopause temperatures near late 1978, which coincides with the introduction of satellite data into the reanalysis. This discontinuity is also evident in reanalysis temperatures throughout upper levels in the tropics [*Pawson and Fiorino*, 2000]. A qualitatively similar but smaller-magnitude discontinuity is found in tropopause pressure anomalies. These discontinuities are not surprising given the importance of satellite data in the reanalysis but clearly limit the usefulness of the data for study of decadal-scale variability. For this reason we focus on interannual variability for the two subperiods 1957-1978 and 1979-1997.

There is a reasonably strong correlation between the radiosonde and NCEP interannual anomalies in Figure 5, with correlation coefficients for the two subperiods of the order of 0.6. Figure 6 shows similar time series of tropopause temperature anomalies at several other stations: Nairobi, Cocos Island, Atuona, and Seawell (Barbados) (see Figure 1). These time series show characteristics similar to the comparisons at Truk (Figure 5), namely, an apparent discontinuity in NCEP data near 1978 and reasonable agreement between the radiosonde and NCEP data for the time period 1979-1997 (although the comparison is not as good at Nairobi, where the correlation coefficient is only 0.34).

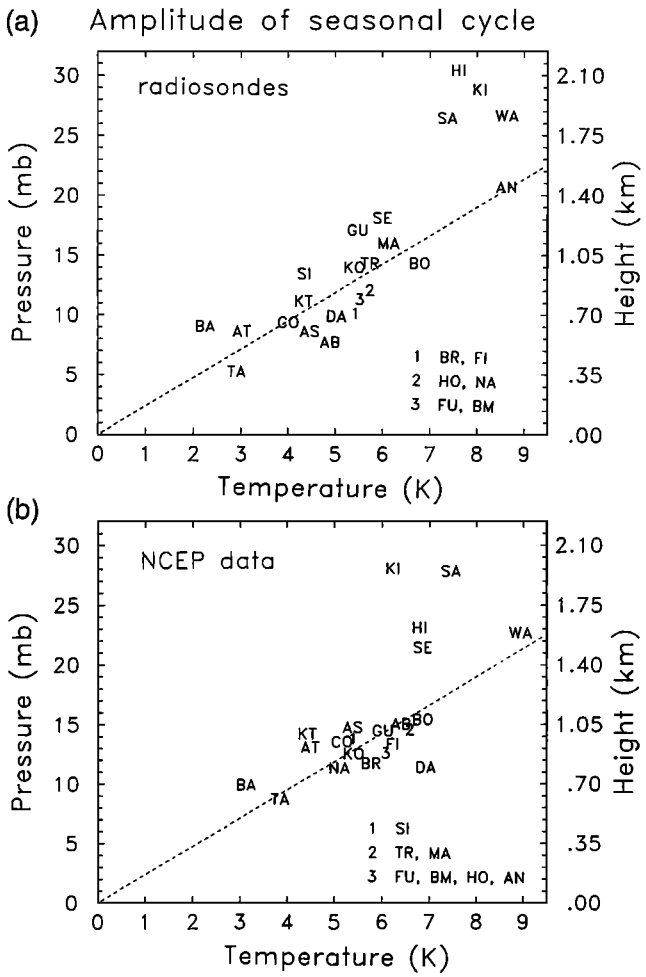

Figure 3. (a) Amplitude of the annual cycle in tropopause temperature and pressure at each radiosonde station, calculated as discussed in the text. For clarity, some station results are indexed numerically. An approximate altitude scale is indicated on the right axis, and the dashed line indicates a slope of 6 K/km. (b) Same as Figure 3a but using NCEP reanalysis data sampled at the radiosonde station locations.

The time series in Figure 6 furthermore serve to illustrate several problems of the historical radiosonde data sets. Although the time series since ~1980 are reasonably complete at most stations, the pre-1980 data have variable length records and can have substantial gaps (e.g., Nairobi). Furthermore, the early time series at many stations show considerably warmer mean temperatures as compared with the latter record (for example, Nairobi prior to ~1975 and Atuona prior to 1976, in Figure 6). These changes are likely associated with one or more changes in radiosonde instrumentation at each station, wherein the earlier instruments had warm biases due to the combined effects of solar radiation impinging on the sensors and long instrument response times. *Gaffen* [1994] found widespread evidence of abrupt changes in radiosonde temperature data at fixed pressure levels due to changes in instruments and methods of observation, so it is not surprising to find comparable problems in tropopause temperature time series. While some effects are easy to detect by visual inspection, such as at Atuona (Figure 6), others are more subtle either because the effect is small or because it is masked by real atmospheric variability. Because temperature trend estimates are very sensitive to the existence and treatment of these data inhomogeneities [*Gaffen et al.*, 2000], and because a thorough analysis of these effects is beyond the scope of this study, our discussion of long-term tropopause temperature changes in these data sets will be limited.

Figure 7 shows the correlation coefficients between radiosonde and NCEP temperature interannual anomalies over 1979-1997 at each station. Values range from 0 34 (Nairobi) to 0.86 (Honolulu), with most values in the range 0.5-0.7. Although these values are statistically significant, they indicate that less than half of the variance is linearly related. On the other hand, correlations between radiosonde statistics at "nearby" stations such as Truk-Koror or Kingston-San Juan only have values of order 0.6-0.8, suggesting significant variability of monthly means at small spatial sales. Inspection of individual time series (e.g., Figures 5 and 6) shows that most of the "large-amplitude" variations during 1979-1997 are accurately captured by the NCEP reanalyses, and this is confirmed below by direct comparisons of space-time variations in both data sets.

4.2. Interannual Signals

4.2.1. Global variability and trends. One important feature of tropopause variability is that interannual fluctuations are

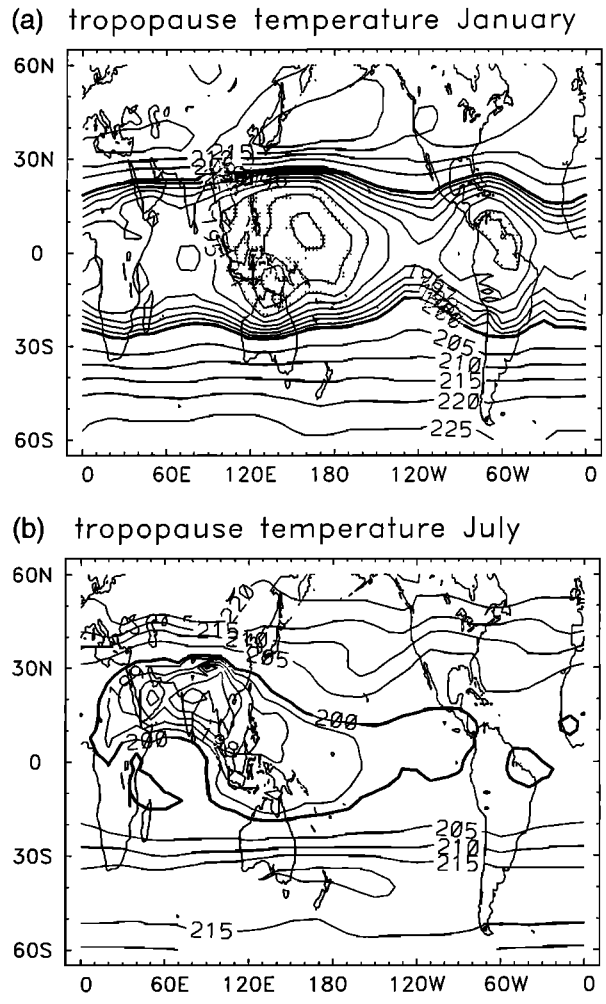

Figure 4. Global tropopause temperature in (a) January and (b) July based on NCEP reanalysis. Contour interval is 5 K above 200 K and 1 K below 200 K. Values below 194 K are shaded in Figure 4a.

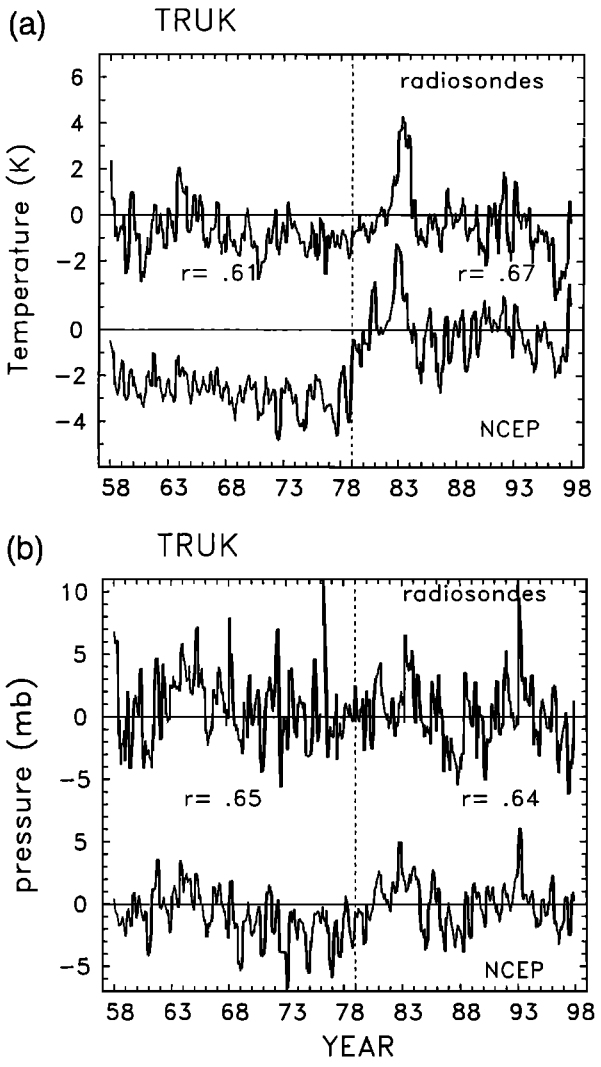

Figure 5. Time series of interannual anomalies in tropopause (a) temperature and (b) pressure at Truk based on radiosondes and NCEP reanalysis data. Correlations between the radiosonde and NCEP data are noted, calculated separately over the periods 1957-1978 and 1979-1997.

substantially smaller than the seasonal cycles in both the tropics and extratropics. This is illustrated in Figure 8, which shows the zonal mean NCEP tropopause temperature over 20°N-S, together with a deseasonalized version of the data. The amplitude of the tropical seasonal cycle is of order ~5 K, whereas interannual variations are of order ±1-2 K. A similar statement is true for tropopause pressure variability: The seasonal cycle is of order 10-15 mbar (Figure 3), while interannual anomalies are ~± 2-4 mbar (Figure 5).

The NCEP tropopause temperature anomalies in Figure 8 show episodic warm periods during 1980-1983 and 1989-1993 of order ~1-2 K, with relative cold periods otherwise. Figure 8 also includes an estimate of radiosonde temperature anomalies averaged over the tropics, using an average of the 12 stations circled in Figure 1. This subsampling of available data was chosen subjectively to provide approximate equal area weighting, given the low density of stations away from Indonesia and the western Pacific Ocean. Estimates using all 26 stations provide means very similar to this 12-station subsample, with rms differences between the two estimates of only 0.35 K. We furthermore sampled the NCEP reanalysis data at these 12 radiosonde locations (dashed line in Figure 8) and found results nearly identical to the zonal means; thus differences between the radiosondes and NCEP means are not due primarily to spatial sampling issues. Comparison of the NCEP and radiosonde anomalies in Figure 8 shows reasonable agreement, but there are two periods of notable differences: 1986-1987, when NCEP data are ~1 K colder, and 1989-1993, when NCEP is warmer by ~1 K. These differences strongly impact estimates of temperature trends over 1979-1997, as discussed in more detail below.

Figure 9 shows deseasonalized tropical average anomalies in tropopause pressure for NCEP and radiosonde data. Interannual variations of order ±3 mbar (~±200 m) are seen, with higher pressures (lower altitudes) associated with warm temperature anomalies in Figure 8. There is reasonable agreement between the NCEP and radiosonde pressure anomalies in Figure 9, with less evidence of the differences for 1986-1987 and 1989-1993 than is seen in temperatures.

The nature of the temperature variations seen in Figure 8, and the NCEP-radiosonde differences, are explored further in Figure 10. Here the tropopause temperature anomalies are shown in conjunction with the mean temperature of the ~150- to 50-mbar layer as measured by the satellite-borne microwave sounding unit (MSU) channel 4, along with the mean tropospheric temperatures over ~1000-200 mbar from MSU channel 2 [*Spencer and Christy*, 1992, 1993]. The MSU4 data show episodic warming of the tropics in 1982-1983 and 1991-1992 attributable to the volcanic eruptions of El Chichón and Pinatubo. These volcanic events were associated with warming primarily in the lower stratosphere, with magnitudes above 3 K [*Labitzke and McCormick*, 1992; *Angell*, 1993]; the vertical weighting of MSU4 produces the 1- to 2-K anomalies seen in Figure 10. The El Chichón warming is evident at the tropopause in both the NCEP and radiosonde data in Figure 10, although the tropopause time series suggest some warming during 1980-1981, prior to the eruption. The effect of Pinatubo is less distinctive at the tropopause, particularly in the radiosonde averages, and it is also difficult to isolate in individual station records (see Figure 6). Furthermore, the 1989-1990 warming seen in NCEP data (but not radiosondes) is not associated with a similar magnitude warming in MSU4 or any clear signal in the lower troposphere (it lags the maximum 1988-1989 ENSO "cold event" by at least a year). Because these 1989-1990 NCEP anomalies are not evident in radiosonde or satellite data directly, we are skeptical of their reality.

The radiosonde and NCEP tropopause temperature anomalies are compared with ECMWF and UKMO data in Figure 11. For direct comparison with the 100-mbar ECMWF and UKMO data, we also include the 100-mbar NCEP temperature anomalies in Figure 11, and these are seen to track the NCEP tropopause statistics nearly identically. The data from ECMWF reanalyses (1979-1993) show relatively little interannual variability compared with the radiosonde and NCEP results; even the 1982-1983 warming is difficult to isolate from ECMWF. This lack of variability makes it difficult to use the ECMWF data to discern biases in the radiosonde or NCEP results for the 1979-1993 period. When the operational ECMWF analyses are included after 1993, a cooling of the tropopause by ~1 K for 1995-1997 is evident (as noted by *Simmons et al.* [1999]). Although the details of the combined ECMWF record are suspect (due to changes in analyses), a similar (but weaker) cooling during the 1990s is evident in the radiosonde, NCEP, and UKMO data.

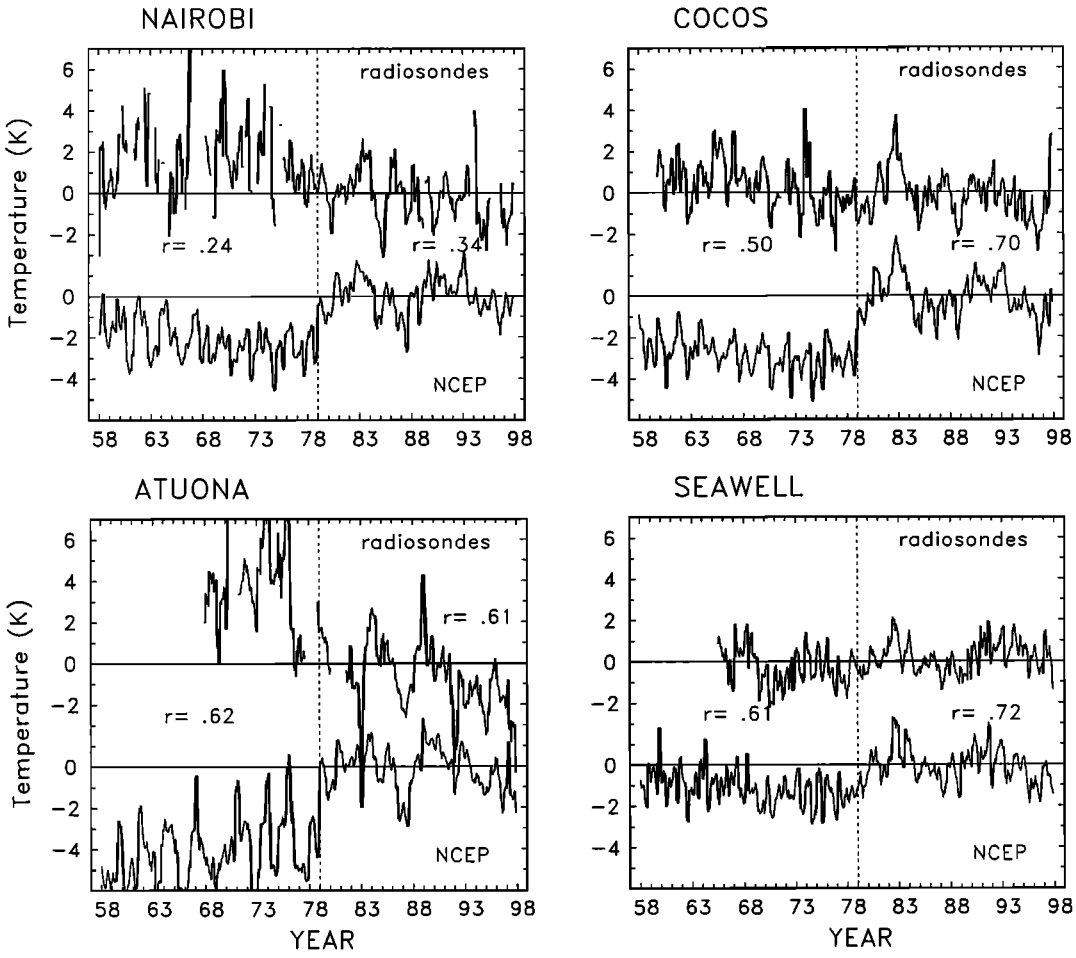

Figure 6. Interannual variations in tropopause temperature at Nairobi, Cocos Island, Atuona, and Seawell, derived from radiosonde and NCEP reanalysis data.

Linear regression of the NCEP reanalysis zonal mean tropopause temperature time series over 20°N-S for the period 1979-1997 gives a linear trend of 0.04 ± 0.22 K/decade, whereas the trend for the 12-station radiosonde average is -0.57 ± 0.18 K/decade (the quoted uncertainties are two sigma standard errors and include statistical but not instrumental uncertainties). The difference in trends arises mainly from the 1986-1987 cold and 1989-1993 warm anomalies seen in NCEP but not radiosonde data in Figures 8-11. Correspondingly, there is an (apparent) significant projection onto the 11-year solar cycle for NCEP data (0.08 ± 0.02 K/100 units of $F10.7$ cm radio flux), but not for the radiosondes (0.01 ± 0.01 K/100 units of $F10.7$). Trends calculated from the combined ECMWF data for 1979-1997 are – 0.61 ± 0.16 K/decade, reduced to –0.29 ± 0.10 K/decade for the shorter 1979-1993 reanalysis period. The solar cycle is not significant in ECMWF data for either period. The magnitude and

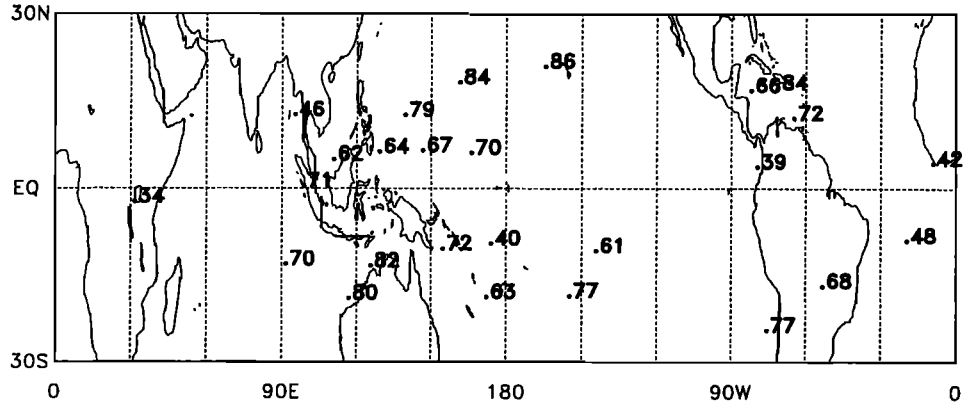

Figure 7. Correlation coefficients between interannual anomalies in tropopause temperature from radiosondes and NCEP reanalyses, for the period 1979-97.

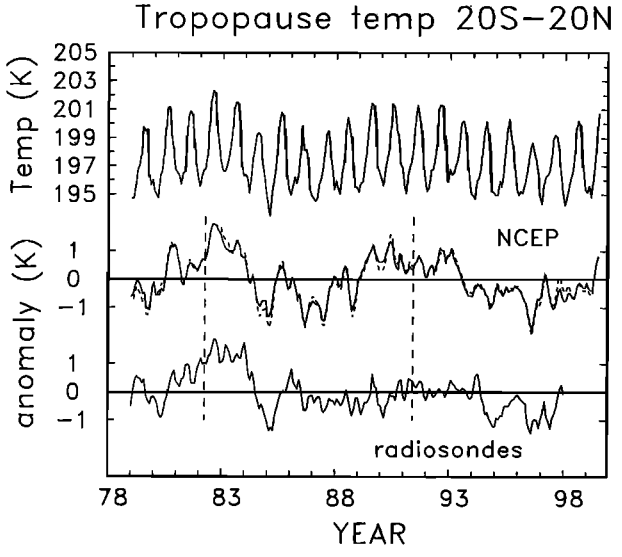

Figure 8. Top region shows a time series of zonal mean tropopause temperatures over 20°N-S from NCEP data during 1979-1999. As discussed in text, these data probably have a warm bias of order ~4 K. Middle region shows interannual anomalies in NCEP tropopause temperature, for zonal means over 20°N-S (solid line). The dashed line, which virtually overlays the solid line, shows the NCEP results sampled/averaged at the 12 radiosonde station locations. Bottom region shows tropical average temperature anomalies for 1979-1997 derived from an average of 12 stations highlighted in Figure 1. Vertical dashed lines denote the eruptions of El Chichón (1982) and Pinatubo (1991).

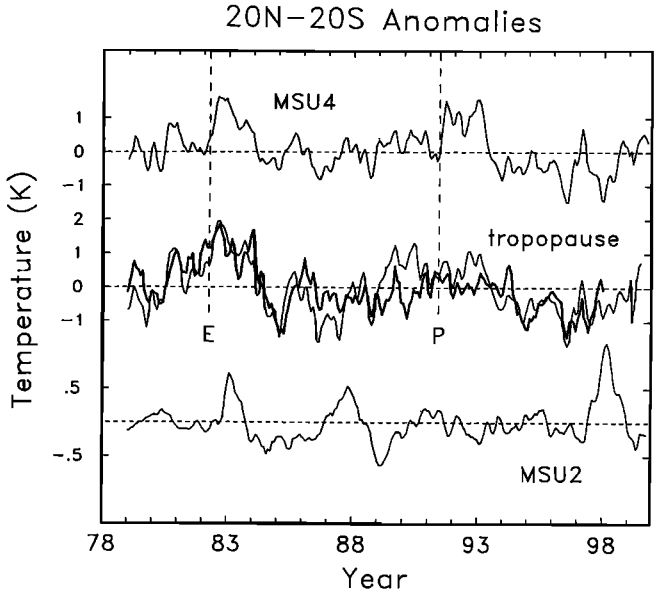

Figure 10. Interannual anomalies in temperature for the 150- to 50-mbar layer (MSU4 data, top curve) and the 1000- to 200-mbar layer (MSU2 data, bottom curve), averaged over 20°N-S. The middle curves are the tropical average tropopause temperature anomalies (as in Figure 8), derived from NCEP (thin curve) and radiosonde data (bold curve). Letters E and P denote the volcanic eruptions of El Chichón and Pinatubo.

significance of the trends in the radiosonde data are affected by the El Chichón warming early in the 1979-1997 record: If the 1982-1983 period is omitted, the trends become less negative (-0.28 ± 0.17 K/decade). The statistically significant negative trend in averaged radiosonde data should be treated cautiously, in light of possible inhomogeneities of the individual radiosonde records.

Trends in tropopause pressure over 1979-1997 for the 20°N-S region (the time series shown in Figure 9) show small values of -0.32 ± 0.52 mbar/decade for the NCEP data and -0.62 ± 0.52 mbar/decade for the radiosondes. However, these small trends

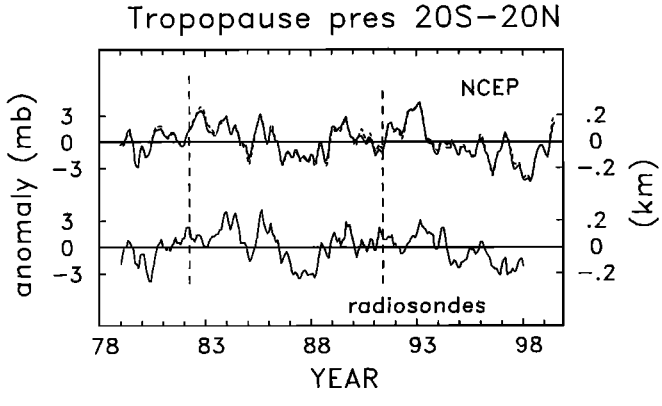

Figure 9. Interannual anomalies in tropical tropopause pressure derived from NCEP reanalysis data (top region) and radiosonde data (bottom region) Details are the same as in Figure 8. An approximate height scale is included on the right axis.

are highly sensitive to removal of the postvolcanic time periods and in any case contain only small fractions of the overall variance.

We note the NCEP tropopause temperatures show a strong negative trend during the presatellite period 1957-1978 (as seen in Figures 5 and 6). However, calculation of the 1958-1978 trends for zonal bands shows nearly constant negative trends from 30°S to the North Pole and strong positive trends south of 50°S. This spatial structure is clearly unrealistic and suggests some problem in the reanalysis tropopause data for 1958-1978, at least for trend-like variations.

4.2.2. QBO. The QBO is a well-known interannual signal observed in tropical tropopause statistics [*Angell and Korshover*, 1964; *Reid and Gage*, 1985]. A QBO variation in tropopause behavior is expected because there is a perturbation in lower stratospheric temperature, which is in thermal wind balance with the QBO zonal wind variations [e.g., *Andrews et al.*, 1987, equation 8.2.2; *Dunkerton and Delisi*, 1985; *Randel and Cobb*, 1994]. QBO temperature anomalies have a symmetrical structure centered over the equator (~10°N-S), with variations of order ±4 K near 30 mbar and ±1 K at 70 mbar [*Dunkerton and Delisi*, 1985; *Pawson and Fiorino*, 1998; *Randel et al.*, 1999a]. Because a relatively large number of QBO cycles are contained in the observational record, it is straightforward to isolate the QBO structure based on regression with observed QBO winds. Tests show that the zonal winds near 50 mbar are best correlated with tropopause temperature and pressure anomalies; this is reasonable because the 50-mbar winds are in thermal wind balance with temperature anomalies in the lowest stratosphere.

Figure 12 shows anomalies in NCEP zonal mean tropopause temperature over the equator for the periods 1958-1978 and 1979-1997, together with the QBO component of variation derived from regression. The statistical QBO signal is of order

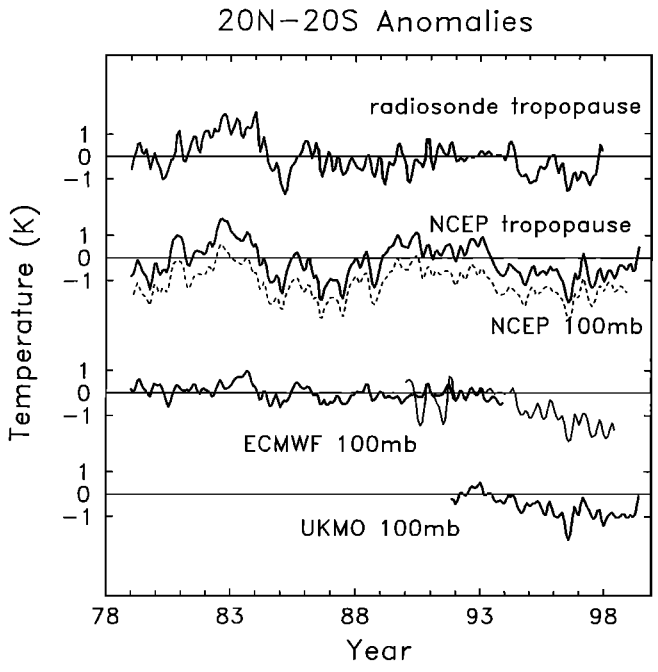

Figure 11. Time series of interannual anomalies in tropopause temperature from radiosondes and NCEP reanalysis data (top two curves), plus 100-mbar temperature results from NCEP (dashed line), European Centre for Medium-Range Weather Forecasts (ECMWF), and United Kingdom Meteorological Office (UKMO) data. The ECMWF results show data from reanalyses (bold curve for 1979-1993) and operational analyses (thin line for 1990-1998). UKMO data are only available since late 1991. All results are averages over 20°N-S.

±0.6 and ±0.3 K for these two samples, with positive tropopause temperatures associated with positive (westerly) QBO winds at 50 mbar. NCEP tropopause temperature anomalies for the 1958-1978 period are dominated by the QBO, which explains 52% of the total variance (although this is probably unrealistically large, as discussed below) In contrast, for the 1979-1997 period the QBO captures a relatively small fraction (12%) of the interannual variance (although it is still a statistically significant component).

Figure 13 shows the latitudinal structure of the QBO variation in tropopause temperature and pressure over 1979-1997 for NCEP data, together with results for each of the 26 radiosonde stations. The NCEP and radiosonde data are in good agreement, showing a maximum near the equator, and negative (out-of-phase) variations in subtropics of each hemisphere, for both temperature and pressure. These out-of-phase subtropical maxima are a characteristic dynamical signature of the QBO [e.g., *Randel et al.*, 1999a] and are clearly observed in lower stratospheric temperature and column ozone data [*Randel and Cobb*, 1994; *Tung and Yang*, 1994]. At the equator, QBO anomalies in zonal mean tropopause pressure are of order ±1 mbar, corresponding to height variations of ~±70 m.

The substantially larger QBO signal seen in the NCEP data for the presatellite period (1958-1978) in Figure 12 is intriguing. Figure 14 shows the latitudinal structure of the derived QBO signal in tropopause temperature for this 1958-1978 period, including results for 22 of the 26 radiosonde stations where the data records were of sufficient length to support a QBO analysis. Comparison with Figure 13 shows that the NCEP data for the 1958-1978 period have much larger QBO magnitude at the equator but that the latitudinal structure is unrealistically broad for this earlier period. In particular, the nodal points near 15°N and 15°S derived for the 1979-1997 period (Figure 13) are in good agreement with satellite temperature observations [*Randel and Cobb*, 1994], whereas the nodes near 20°-25°N and 20°-25°S for the 1958-1978 period in Figure 14 are unrealistic. Furthermore, comparison with the radiosonde QBO statistical estimates in Figure 14 shows that NCEP data overestimates the QBO amplitude at a majority of stations. Together these pieces of evidence suggest that the QBO variability in NCEP data for 1958-1978 is too large and not correct in detail, whereas the 1979-1997 results appear more reasonable.

4.2.3. ENSO. *Reid and Gage* [1985] and *Gage and Reid* [1987] report evidence of ENSO variations in tropical tropopause height and temperature. In particular, *Gage and Reid* [1987] demonstrate that the ENSO signature is primarily associated with longitudinal variations over the western Pacific Ocean. This is consistent with *Yulaeva and Wallace* [1994], who show that the ENSO signal in lower stratospheric temperature is primarily evident in zonal variations in the tropics. Indeed, the tropical average tropopause statistics here (Figures 8-10) do not show obvious coherence with ENSO events (which are evident in the MSU2 data in Figure 10). Thus, following *Yulaeva and Wallace* [1994], we isolate the ENSO signal in tropopause data by first removing the zonal mean component at all latitudes. Regression

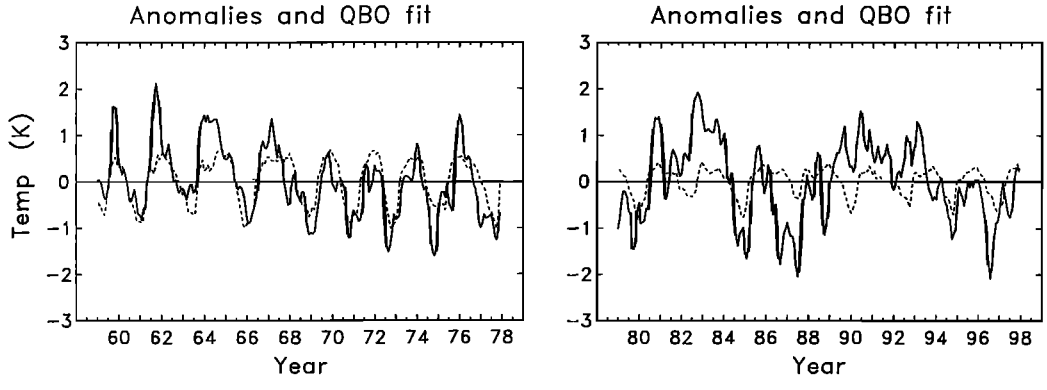

Figure 12. Time series of NCEP interannual anomalies in tropopause temperature at the equator (solid curves), together with the quasi-biennial oscillation (QBO) component derived from regression analysis (dashed curves). Results are shown for the 1958-1978 and 1979-1997 periods separately.

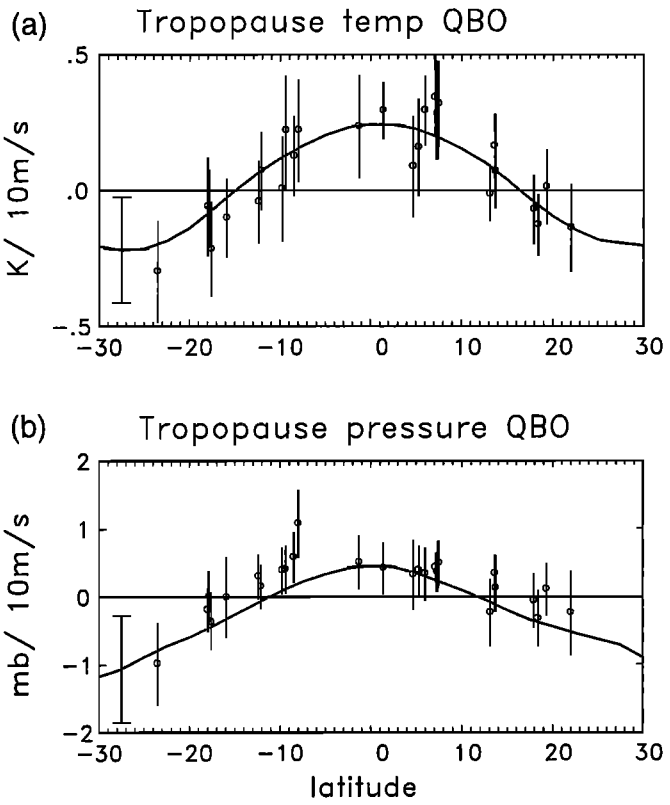

Figure 13. Latitudinal structure of the QBO variation in tropopause (a) temperature and (b) pressure for 1979-1997, derived from regression analysis. Curves show NCEP data, and circles indicate results for each radiosonde location. Error bars indicate $\pm 2\sigma$ statistical uncertainties. Units are kelvins or millibars per 10 m/s of QBO winds at 50 mbar, which vary over ~±20 m/s during a QBO cycle.

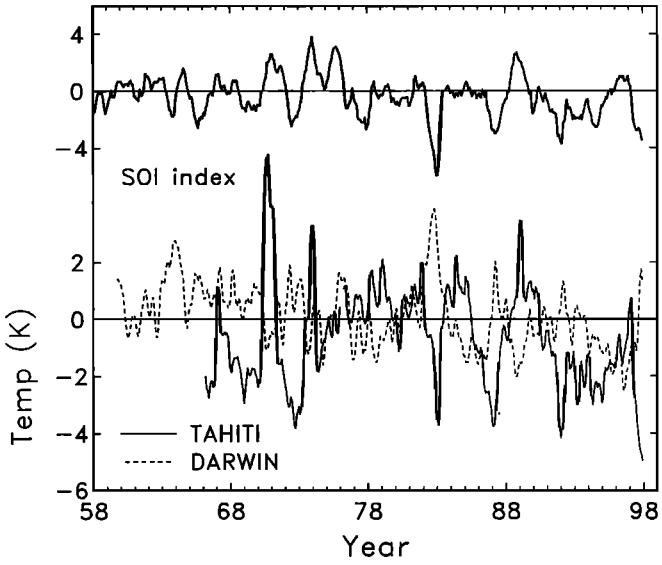

Figure 15. Top curve shows time series of the normalized Southern Oscillation Index (the difference between Darwin and Tahiti surface pressure). Bottom curves show tropopause temperature anomalies at Darwin (dashed) and Tahiti (solid). The Tahiti data have a discontinuity (of 6.3 K) in 1976 that has been removed here by equating the time means before and after 1976.

analyses use the standardized ENSO or Southern Oscillation Index (SOI) shown in Figure 15. We note that the removal of zonal means also helps separate the volcanic and ENSO signals, because although there is some temporal overlap of ENSO and volcanic events in 1982-1983 and 1991-1992, the volcanic signal is primarily a zonal mean effect.

The spatial patterns of tropopause temperature from the NCEP reanalysis regressed upon the ENSO index are shown in Figure 16 for both 1958-1978 and 1979-1997 time periods; the regressions are shown for data over December-March, when the ENSO signal is maximum [*Yulaeva and Wallace,* 1994]. A remarkably similar pattern is seen in both subperiods, with an east-west dipole pattern centered in the western Pacific and symmetric ("dumbbell-shaped") maxima slightly north and south of the equator. The positive maxima centered near 140°W correspond to tropopause cooling during ENSO "warm events," (negative extrema of SOI in Figure 15), and likewise the tropopause is relatively warm near 140°E. ENSO warm events are associated with a warming in eastern Pacific sea surface temperatures, a shifting of convection from Indonesia toward the east, and warming of the global tropical troposphere (see the MSU2 time series in Figure 10). The tropospheric warming exhibits local maxima in the central Pacific very similar to the positive contours seen in Figure 16, and these patterns are mirrored in lower stratospheric cooling patterns [*Yulaeva and Wallace*, 1994]. The tropopause temperature anomalies thus have opposite sign to tropospheric temperatures and the same sign as stratospheric anomalies. The dumbbell-shaped temperature maxima symmetric about the equator are signatures of a pair of cyclonic vorticity maxima slightly to the east of the anomalous heating, and these tropopause anomalies are consistent with idealized model calculations [e.g., *Gill*, 1980; *Highwood and Hoskins*, 1998]. While these patterns are not unexpected for the 1979-1997 period (given the similar results of *Yulaeva and Wallace* [1994], based on satellite data), it is remarkable to observe such details in the presatellite data period, because of the lack of dense radiosonde network in the eastern Pacific. Apparently, the available data (including sea surface temperatures) combine with the assimilation model physics to produce realistic spatial anomaly structures. Similar spatial structures are derived for ENSO tropopause pressure variations (not shown), with typical values of ± 0.3-0.6 mbar/SOI.

The network of radiosonde datas show a longitudinal structure to ENSO that is very similar to NCEP results. Figure 17 shows the ENSO regression coefficients for each radiosonde station for

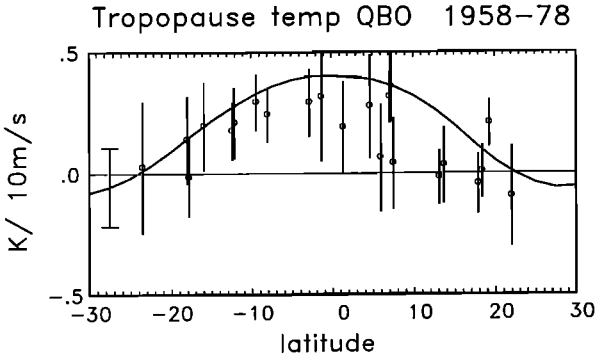

Figure 14. Latitudinal structure of QBO variations in tropopause temperature for 1958-1978. Details are the same as Figure 13.

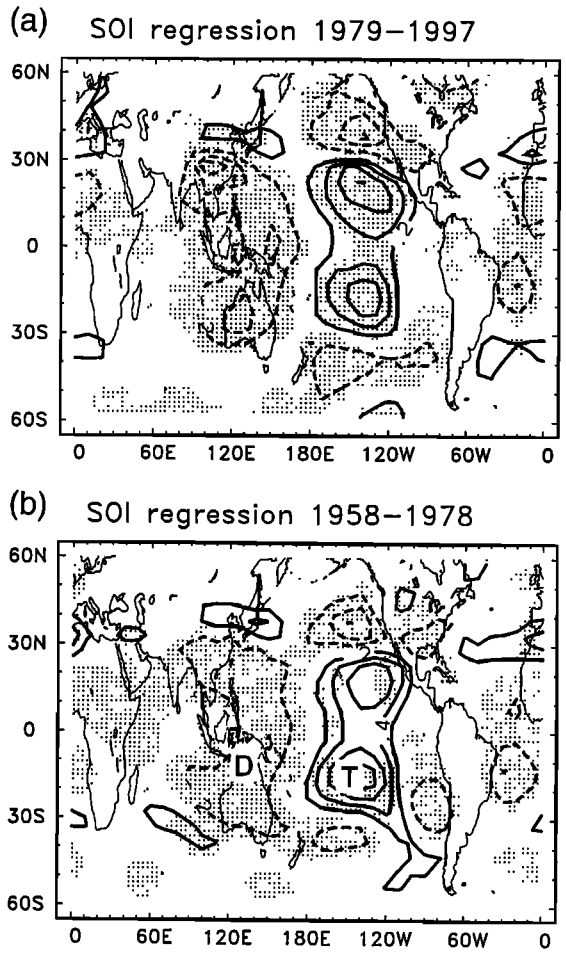

Figure 16. Spatial patterns of El Nino-Southern Oscillation (ENSO) variations in tropopause temperature during December-March derived from regression analysis on the Southern Oscillation Index (SOI) in Figure 15. Contour interval is 0.2 K per SOI value, and zero contours are not shown. Zonal mean values were removed prior to these calculations. Results are shown separately for the (a) 1958-1978 and (b) 1979-1997 time periods. Stippled areas represent 95% statistical significance. The locations of Darwin (D) and Tahiti (T) are indicated in Figure 16b.

the period 1979-1997, together with the NCEP results (over 10°-20°S). Large positive coefficients are observed in the central Pacific region (at Honolulu, Tahiti and Atuona; see Figure 1), in spatial agreement with NCEP results. Likewise, negative coefficients are found (for temperature) for most stations over 90°-160°E. The ENSO signal is clearly demonstrated in time series of tropopause temperature anomalies at Darwin and Tahiti, shown in Figure 15 which are located near the centers of the east-west dipole patterns in Figure 16. These time series show coherent out-of-phase variations in tropopause temperature for the record extending back to the 1960s. We note that the surface pressure differences between Darwin and Tahiti are often used as a standard reference for ENSO variability [e.g., *Trenberth*, 1984]; the data here show that ENSO can also be easily identified in tropopause statistics at these same stations.

4.3. Coherence With Extratropics

The correlation between variability of the tropical tropopause and circulation in the extratropics can provide further information on mechanisms of tropical variability. Coherent variations of the tropical tropopause and the extratropical stratospheric circulation may be anticipated due to variations of the stratospheric Brewer-Dobson circulation [*Holton et al.*, 1995; *Reid and Gage*, 1996]. Here we examine the latitudinal and seasonal behavior of tropical-extratropical relationships by calculating interannual correlations between NCEP tropopause temperatures (over 20°N-S) and zonal mean 100-mbar temperatures at each latitude The interannual correlations shown in Figure 18 are calculated for each individual month, separately for the two time periods 1958-1978 and 1979-1997 (because of the discontinuity in tropical statistics across 1978-1979). Because the space-time correlation patterns are very similar for each 20-year sample, we average the results to obtain a more stable statistical estimate. Treating each year as independent (i.e., approximately 38 degrees of freedom over 1958-1997 for each monthly calculation), a correlation coefficient of 0.31 is statistically significant at the 95% confidence level.

The spatial pattern of correlations shown in Figure 18 reveal significant positive values over approximately 45°N-S, with high values (>0.9) over ~20°N-S (as expected, since the tropopause is very close to 100 mbar). Most interesting in the results of Figure 18 are patterns of significant negative correlation for NH polar regions during winter-spring (December-March) and SH high latitudes (50°-70°S) during late winter-spring (August-October). These correlations demonstrate an out-of-phase relationship between the tropical tropopause and the lower stratospheric polar vortex; a scatter diagram showing this anticorrelation for January temperatures is shown in Figure 19. In balance with the latitudinal temperature gradients implied by Figure 18 are

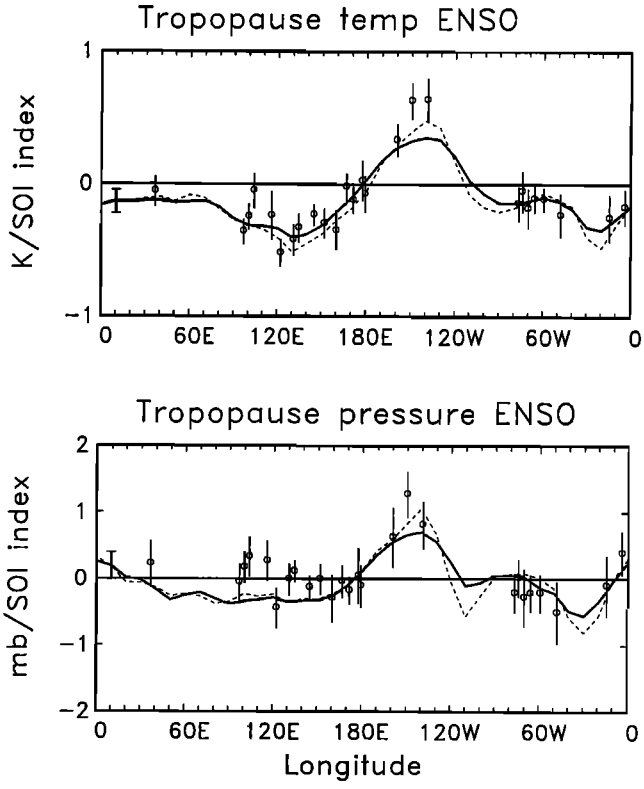

Figure 17. Longitudinal structure of ENSO variations derived from regression analysis over 1979-1997. Solid lines show NCEP results over 10°-20°S for the annual mean; dashed lines are for December-March averages only. Circles show annual mean results for each radiosonde station.

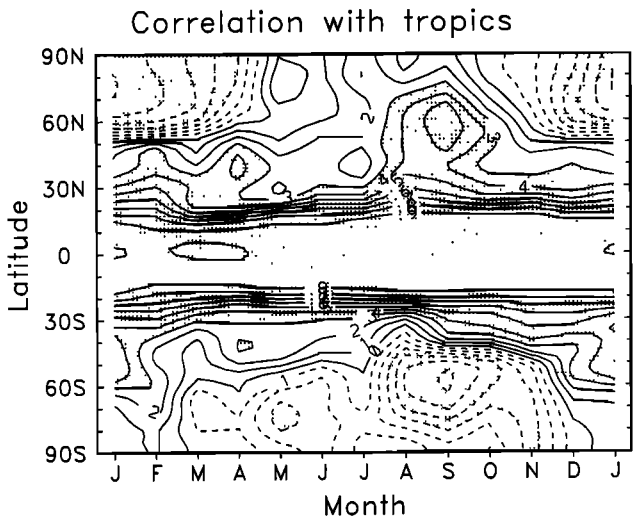

Figure 18. Latitude-time plot of interannual correlations between NCEP reanalysis tropopause temperature averaged over 20°N-S, and 100-mbar zonal mean temperatures at each latitude. These results are an average of calculations over the periods 1958-1978 and 1979-1997.

correlated variations in polar jet intensity, with stronger winds associated with warm tropopause anomalies. Although we have not diagnosed the stratospheric Brewer-Dobson circulation explicitly, the seasonal dependence (maxima in winter-spring) and out-of-phase latitudinal structures seen in Figure 18 are consistent with both the tropics and polar vortex responding to variations of the mean stratospheric circulation, i.e., enhanced tropical upwelling (adiabatic cooling) balanced by stronger polar descent (heating) [see *Holton et al.*, 1995]. The slight NH-SH differences seen in Figure 18 are furthermore consistent with differences in climatological mean downward circulation between the hemispheres: In the NH the maximum is over polar regions, while it is over the 50°-70°S "collar" region in the SH [*Schoeberl et al.*, 1992].

The NH winter polar patterns seen in Figure 18, with a change of phase near 50°N, are furthermore suggestive of correlations with the stratospheric component of the Arctic Oscillation (AO) of *Thompson and Wallace* [1998]. Correlations between the monthly AO index (provided by D. Thompson, personal communication, 1999) and tropopause temperature give significant values of ~0.4-0.6, similar to the 100-mbar polar temperature correlations in Figure 18. *Thompson and Wallace* [2000] note this correlation between the AO and the tropical tropopause and furthermore quantify the associated global wind and temperature variations (their Figure 8). One interesting detail is that while extratropical temperature correlations are apparent only in the stratosphere, significant zonal wind anomalies extend all the way to the surface.

5. Summary and Discussion

Although the model used in the NCEP reanalysis has only ~2-km vertical resolution in the region of the tropopause, comparisons with tropical radiosonde data show that the NCEP tropopause statistics exhibit reasonable seasonal and interannual variability. There are substantial biases in NCEP tropopause temperature in the tropics, with analyses 3-5 K warmer than radiosondes; there is no strong spatial structure to these biases. Likewise, there are biases of ~2-6 mbar in tropical tropopause pressure (with NCEP too high in pressure or too low in altitude). Both the temperature and pressure biases are approximately constant during the year, so that the NCEP seasonality is realistic. There is a substantial discontinuity in the NCEP tropopause data between the presatellite and postsatellite data period, consistent with previously noted temperature discontinuities.

Interannual anomalies in tropically averaged NCEP and radiosonde statistics during 1979-1997 show variations of order ±1-2 K and ±3 mbar for temperature and pressure, respectively. Although there are periods of good agreement, there are extended times when differences between the NCEP and radiosondes are of order 1 K (see Figure 10). Time series of 100-mbar temperatures from ECMWF reanalyses (1979-1993) show much reduced variability and substantial differences compared to both radiosondes and NCEP (Figure 11). Thus these three estimates of tropical tropopause variability exhibit differences which are of similar magnitude to the variability itself, and this has substantial effects on estimates of decadal trends, for example. Differences between these analyses are one measure of the uncertainty of our current understanding of decadal variability of the tropopause.

Linear trends calculated for the period 1979-1997 show significant negative temperature trends for the 12-station average radiosonde data, with magnitude of –0.57 ± 0.18 K/decade. A large part of this trend comes from the El Chichón anomaly early in the record; omission of the 1982-1983 data drops the radiosonde trends to – 0.28 ± 0.17 K/decade. NCEP data for 1979-1997 do not exhibit statistically significant trends (0.04 ± 0.22 K/decade). ECMWF reanalyses have trends of – 0.29 ± 0.10 K/decade for 1979-1993, increased to – 0.61 ± 0.16 K/decade if operational analyses are appended over 1994-1997. Each data set shows the period 1994-1997 to be relatively cold, although similar cool periods were observed in the 1980s in both radiosonde and NCEP data. There is a statistically significant projection of the 11-year solar cycle found in the NCEP reanalyses, but no such signal is found using radiosondes or ECMWF results.

In spite of the differences noted above, there are several coherent signals which are evident in both the radiosonde and

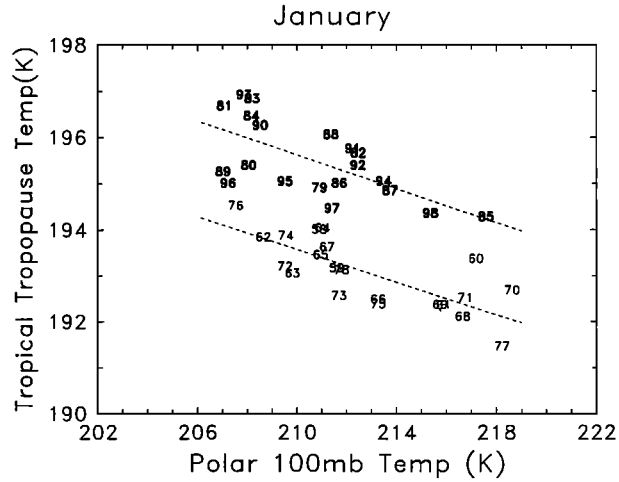

Figure 19. Scatterplot of tropopause temperature (20°N-S) versus Northern Hemisphere polar temperature at 100 mbar (60°-90°N) for January averages. Individual years are noted numerically (79 = 1979, etc.), with darker symbols for the 1979-1998 period. The dashed lines are regression slopes for the two periods.

NCEP tropopause data. The volcanic eruption of El Chichón in 1982 is associated with a zonal mean warming of the tropical tropopause temperature by ~1-2 K, and a decrease in altitude by ~200 m, which lasts for approximately 1-2 years. Although Mount Pinatubo in 1991 was a larger volcanic eruption [*Coffey*, 1996] and produced equal or larger warming in the lower stratosphere, its effects are less apparent in tropopause anomalies, particularly as observed by radiosondes. Part of this difference could be attributable to El Chichón occurring just prior to the QBO westerly shear phase (warm temperatures), whereas Pinatubo erupted before an easterly (cool) phase (see Figure 12); thus the volcanic and QBO effects reinforce for El Chichón and partially cancel for Pinatubo [*Angell*, 1997].

Recent observational studies suggest evidence of increasing water vapor in the stratosphere [*Oltmans and Hofmann*, 1995; *Nedoluha et al.*, 1998; *Randel et al.*, 1999b]. One mechanism for such an increase could be a temporal increase in tropical tropopause temperature or a decrease in pressure (increase in height), which could allow larger saturation mixing ratios to enter the stratosphere. The approximate increase in stratospheric water vapor from the above references is of order 1%/yr, or a mixing ratio trend of ~0 07 ppmv/yr For background conditions of T ~ 193 K and p ~ 100 mbar, such a change in saturation mixing ratio corresponds to a temperature increase of ~0.1 K/yr (at constant pressure) or a pressure decrease of ~-1.5 mbar/yr (at constant temperature). The tropopause radiosonde data analyzed here suggest a decreasing trend in temperature over the period 1979-1997, inconsistent with increasing stratospheric water vapor. Furthermore, although the NCEP and radiosonde average data indicate a decreasing trend in tropopause pressure, the observed values of ~-0.3 to -0.6 mbar/decade are more than an order of magnitude smaller than the -1.5 mbar/yr quoted above. We conclude that the observed tropical average tropopause statistics for 1979-1997 are not consistent with an increase in stratospheric water vapor entering across the tropical tropopause. One caveat is that the tropical "cold-point" tropopause is probably more directly related to water vapor entry into the stratosphere than the thermal lapse rate tropopause analyzed here, and further work is needed to quantify variability of the cold-point tropopause. There could also be strong spatial structure to the trends which are obscured in our tropical average analyses, but such patterns are not evident in the NCEP data (not shown here).

The tropopause data here reveal the QBO and ENSO variability documented previously [*Reid and Gage*, 1985; *Gage and Reid*, 1987]. The QBO signal shows near-equatorial tropopause temperature and pressure anomalies of order 0.5 K and 1 mbar, respectively, which are in-phase with the QBO zonal winds near 50 mbar (as expected from thermal wind balance). Oppositely signed QBO variations are observed in the subtropics, so that there are relatively small QBO variations for the tropics averaged over ~ 30°N-S. The QBO signal in NCEP reanalyses for the period 1958-1978 (prior to inclusion of satellite data) is found to have too large amplitude (compared to radiosondes) and an unrealistically broad meridional structure. While the QBO signal is primarily a zonal mean feature, the ENSO variations in tropopause statistics are most evident in deviations from the zonal mean. ENSO tropopause variations are evident as an east-west seesaw over the western and central Pacific ocean with local maximum anomalies of order ±2-3 K and ±4-6 mbar for temperature and pressure, respectively. The derived spatial patterns (Figure 16) are similar to ENSO variations in tropospheric and lower stratospheric temperatures [*Yulaeva and Wallace*, 1994] and the results of idealized model simulations [*Gill*, 1980; *Highwood and Hoskins*, 1998]. Tropopause temperature anomalies are out of phase with tropospheric temperatures and in phase with the lower stratosphere. A surprising result is that realistic ENSO spatial anomalies are observed over data-sparse oceanic regions during the presatellite era (1958-1978), suggesting this feature is reasonably well depicted by the model when other data sources are available.

Finally, we find significant (negative) correlations between interannual variations of the tropical tropopause and lower stratospheric temperatures in both polar regions during winter-spring. The out-of-phase behavior is consistent with variations of the mean stratospheric (Brewer-Dobson) circulation, wherein tropical upwelling is balanced with polar descent. These correlations suggest that stratospheric circulation is an important factor in tropical tropopause variability, as previously argued from observations of the seasonal cycle [e.g., *Reid and Gage*, 1996].

Acknowledgments. We thank Jim Angell, J. F Lamarque, Steve Massie, Phil Mote, and two anonymous reviewers for constructive comments on this paper. Marilena Stone expertly prepared the manuscript. This work was partially supported by NASA grants W-18181 and W-16215 The National Center for Atmospheric Research is operated by the University Corporation for Atmospheric Research under the sponsorship of the National Science Foundation

References

Andrews, D G., J R. Holton, and C. B Leovy, *Middle Atmosphere Dynamics*, 489 pp., Academic, San Diego, Calif., 1987

Angell, J K , Comparison of stratospheric warming following Agung, El Chichón, and Pinatubo volcanic eruptions, *Geophys. Res. Lett , 20*, 715-718, 1993.

Angell, J. K , Stratospheric warming due to Agung, El Chichón, and Pinatubo taking into account the quasi-biennial oscillation, *J. Geophys. Res., 102*, 9479-9485, 1997.

Angell, J. K., and J. Korshover, Quasi-biennial variations in temperature, total ozone, and tropopause height, *J Atmos. Sci., 21*, 479-492, 1964

Brewer, A. W., Evidence for a world circulation provided by the measurements of helium and water vapor distribution in the stratosphere, *Q. J .R. Meteorol Soc , 75*, 351-363, 1949.

Coffey, M. T., Observations of the impact of volcanic activity on stratospheric chemistry, *J. Geophys. Res , 101*, 6767-6780, 1996

Dessler, A. E., A reexamination of the "stratospheric fountain" hypothesis, *Geophys Res Lett., 25*, 4165-4168, 1998.

Dunkerton, T. J , and D. P Delisi, Climatology of the equatorial lower stratosphere, *J. Atmos Sci , 42*, 376-396, 1985.

Fredrick, J., and A Douglass, Atmospheric temperatures near the tropical tropopause: Temporal variations, zonal asymmetry and implications for stratospheric water vapor, *Mon. Weather Rev., 111*, 1397-1403, 1983.

Gaffen, D J , Temporal inhomogeneities in radiosonde temperature records, *J. Geophys. Res., 99*, 3667-3676, 1994

Gaffen, D. J., M. A Sargent, R. E. Habermann, and J R Lanzante, Sensitivity of tropospheric and stratospheric temperature trends to radiosonde data quality, *J. Clim.*, in press, 2000

Gage, K., and G Reid, Longitudinal variations in tropical tropopause properties in relation to tropical convection and ENSO events, *J. Geophys. Res., 92*, 14,197-14,203, 1987.

Gibson, J K , P Kallberg, S. Uppala, A. Hernandez, A. Nomura, and E Serrano, ERA description, Reanalysis Project Rep. 1, Eur Cent for Medium-Range Weather Forecasts, Reading, England, 1997.

Gill, A E., Some simple solutions for heat-induced tropical circulations, *Q. J. R. Meteorol. Soc., 106*, 447-462, 1980.

Hack, J. J., J. T. Kiehl, and J. W. Hurrell, The hydrologic and thermodynamic characteristics of the NCAR CCM3, *J. Clim., 11*, 1179-1206, 1998.

Hamilton, K., R. J Wilson, J. D. Mohlman, and L. J. Umscheid,

Climatology of the SKYHI troposphere-stratosphere-mesosphere general circulation model, *J. Atmos. Sci., 52*, 5-43, 1995.

Highwood, E J , and B. J. Hoskins, The tropical tropopause, *Q J. R. Meteorol. Soc., 124*, 1579-1604, 1998.

Hoerling, M. P , T D. Schaack, and A. J. Lenzen, Global objective tropopause analysis, *Mon Weather Rev., 119*, 1816-1831, 1991.

Hoinka, K. P , Statistics of the global tropopause pressure, *Mon Weather Rev., 126*, 3303-3325, 1998.

Holton, J., P Haynes, M. McIntyre, A. Douglass, R Rood, and L. Pfister, Stratosphere-troposphere exchange, *Rev Geophys., 33*, 403-439, 1995.

Kalnay, E , et al., The NCEP/NCAR 40-year reanalysis project, *Bull. Am Meteorol Soc , 77*, 437-471, 1996.

Kanamitsu, M , R. E. Kistler, and R W. Reynolds, NCEP/NCAR reanalysis and use of satellite data, *Adv. Space Res , 19(1)*, 481-489, 1997.

Krishna Murthy, B. V., K Parameswaran, and K. O. Rose, Temporal variations of the tropical tropopause characteristics, *J Atmos Sci , 43*, 914-922, 1986

Labitzke, K., and M. P. McCormick, Stratospheric temperature increases due to Pinatubo aerosols, *Geophys. Res. Lett , 19*, 207-210, 1992.

Mo, K. C., Y L. Wang, R. Kistler, M. Kanamitsu, and E. Kalnay, Impact of satellite data on the CDAS-reanalysis system, *Mon. Weather Rev , 123*, 124-139, 1995.

Mote, P., K. Rosenlof, M. McIntyre, E Carr, J Gille, J. Holton, J Kinnersley, H. Pumphrey, J. M. Russell III, and J Waters, An atmospheric tape recorder: The imprint of tropical tropopause temperatures on stratospheric water vapor, *J. Geophys Res., 101*, 3989-4006, 1996.

Naujokat, B., An update of the observed quasi-biennial oscillation of the stratospheric winds over the tropics, *J. Atmos. Sci., 43*, 1873-1877, 1986

Nedoluha, G E., R. M. Bevilacqua, R. M Gomez, D. E. Siskind, B. C. Hicks, J. M. Russell III, and B. J. Connor, Increases in middle atmospheric water vapor as observed by the Halogen Occultation Experiment and the ground-based Water Vapor Millimeter-Wave Spectrometer from 1991 to 1997, *J. Geophys. Res., 103*, 3531-3543, 1998

Newell, R , and S Gould-Stewart, A stratospheric fountain?, *J Atmos. Sci., 38*, 2789-2796, 1981

Oltmans, S. J., and D J Hofmann, Increase in lower-stratospheric water vapor at a midlatitude Northern Hemisphere site from 1981 to 1994, *Nature, 374*, 146-149, 1995.

Pawson, S , and M Fiorino, A comparison of reanalyses in the tropical stratosphere, part 1, Thermal structure and the annual cycle, *Clim. Dyn., 14*, 631-644, 1998.

Pawson, S , and M. Fiorino, A comparison of reanalyses in the tropical stratosphere, part 3, Inclusion of the pre-satellite data era, *Clim. Dyn , 15*, in press, 2000.

Randel, W. J , and J. B Cobb, Coherent variations of monthly mean total ozone and lower stratospheric temperature, *J. Geophys. Res., 99*, 5433-5447, 1994

Randel, W J , F Wu, R Swinbank, J. Nash, and A O'Neill, Global QBO circulation derived from UKMO stratospheric analyses, *J. Atmos Sci., 56*, 457-474, 1999a.

Randel, W J , F. Wu, J M Russell III, and J. Waters, Space-time patterns of trends in stratospheric constituents derived from UARS measurements, *J. Geophys. Res., 104*, 3711-3727, 1999b.

Reid, G., and K Gage, On the annual variation in height of the tropical tropopause, *J Atmos Sci., 38*, 1928-1938, 1981

Reid, G., and K Gage, Interannual variations in the height of the tropical tropopause, *J Geophys. Res., 90*, 5629-5635, 1985.

Reid, G., and K. Gage, The tropical tropopause over the western Pacific: Wave driving, convection, and the annual cycle, *J Geophys. Res., 101*, 21,233-21,241, 1996.

Santer, B. D., et al , Uncertainties in observationally based estimates of temperature change in the free atmosphere, *J. Geophys. Res., 104*, 6305-6333, 1999.

Schoeberl, M. R , L. R. Lait, P. A. Newman, and J. E Rosenfield, The structure of the polar vortex, *J. Geophys. Res., 97*, 7859-7882, 1992

Selkirk, H C., The tropopause cold trap during STEP/AMEX 1987, *J. Geophys. Res , 98*, 8591-8610, 1993.

Simmons, A J , A Untch, C. Jacob, P. Kallberg, and P. Unden, Stratospheric water vapor and tropical tropopause temperatures in ECMWF analyses and multi-year simulations, *Q. J R. Meteorol. Soc., 125*, 353-386, 1999.

Spencer, R W , and J R Christy, Precision and radiosonde validation of satellite gridpoint temperature anomalies, part I, MSU channel 2, *J. Clim., 5*, 847-857, 1992

Spencer, R W , and J. R Christy, Precision lower stratospheric temperature monitoring with the MSU: Technique, validation and results 1979-1991, *J Clim , 6*, 1194-1204, 1993.

Swinbank, R , and A. O'Neill, A stratosphere-troposphere data assimilation system, *Mon. Weather Rev., 122*, 686-702, 1994.

Thompson, D W J., and J. M. Wallace, The Arctic oscillation signature in the wintertime geopotential height and temperature fields, *Geophys Res. Lett., 25*, 1297-1300, 1998

Thompson, D W J , and J. M. Wallace, Annular modes in the extratropical circulation, part I, Month-to-month variability, *J. Clim.*, in press, 2000

Thuburn, J., and G C Craig, GCM tests of theories for the height of the tropopause, *J Atmos. Sci., 54*, 869-882, 1997.

Thuburn, J., and G. C. Craig, Stratospheric influence on tropopause height: The radiative constraint, *J. Atmos. Sci., 57*, 17-28, 2000.

Trenberth, K. E., Signal versus noise in the Southern Oscillation, *Mon Weather Rev., 112*, 326-332, 1984

Tuck, A. F., et al., The Brewer-Dobson circulation in the light of high-altitude in situ aircraft observations, *Q. J. R. Meteorol. Soc., 123*, 1-69, 1997.

Tung, K. K., and H Yang, Global QBO in circulation and ozone, part I, Reexamination of observational evidence, *J. Atmos. Sci., 51*, 2699-2707, 1994

van Loon, H., and K. Labitzke, The 10-12-year atmospheric oscillation, *Meteorol. Z , 3*, 259-266, 1994.

Wallis, T W R , A subset of core stations from the Comprehensive Aerological Reference Dataset (CARDS), *J. Clim., 11*, 272-282, 1998.

World Meteorological Organization, Meteorology – A three-dimensional science· Second session of the commission for aerology, *WMO Bull , IV*, (4), 134-138, 1957

World Meteorological Organization, Measurements of upper air pressure, temperature, and humidity, in *Guide to Meteorological Instruments and Methods of Observation*, 6th ed. chap. 12 *WMO 8*, Geneva, 1996.

Yulaeva, E., and J. M. Wallace, The signature of ENSO in global temperature and precipitation fields derived from the microwave sounding unit, *J. Clim., 7*, 1719-1736, 1994.

D. J Gaffen, NOAA Air Resources Laboratory, Silver Spring, MD 20910.

W. J. Randel and F. Wu, Atmospheric Chemistry Division, National Center for Atmospheric Research, P.O. Box 3000, Boulder, CO 80307-3000. (randel@ucar.edu)

(Received September 3, 1999; revised January 27, 2000; accepted February 29, 2000.)